



Published in final edited form as:

Exp Hematol. 2015 December ; 43(12): 1031–1046.e12. doi:10.1016/j.exphem.2015.08.013.

FANCA safeguards interphase and mitosis during hematopoiesis *in vivo*

Zahi Abdul-Sater^{1,2}, Donna Cerabona^{1,2}, Elizabeth Sierra Potchanant¹, Zejin Sun¹, Rikki Enzor¹, Ying He¹, Kent Robertson¹, W. Scott Goebel¹, and Grzegorz Nalepa^{1,2,3,4,*}

¹Department of Pediatrics, Herman B Wells Center for Pediatric Research, Indiana University School of Medicine, Indianapolis, Indiana, USA.

²Department of Biochemistry and Molecular Biology, Indiana University School of Medicine, Indianapolis, Indiana, USA.

³Department of Medical and Molecular Genetics, Indiana University School of Medicine, Indianapolis, Indiana, USA.

⁴Division of Pediatric Hematology-Oncology, Bone Marrow Failure Program, Riley Hospital for Children, Indianapolis, Indiana, USA.

Abstract

Fanconi anemia (FA/BRCA) signaling network controls multiple genome-housekeeping checkpoints, from interphase DNA repair to mitosis. The *in vivo* role of abnormal cell division in FA remains unknown. Here, we quantified the origins of genomic instability in FA patients and mice *in vivo* and *ex vivo*. We found that both mitotic errors and interphase DNA damage significantly contribute to genomic instability during FA-deficient hematopoiesis and in non-hematopoietic human and murine FA primary cells. Super-resolution microscopy coupled with functional assays revealed that FANCA shuttles to the pericentriolar material (PCM) to regulate spindle assembly at mitotic entry. Loss of FA signaling rendered cells hypersensitive to spindle chemotherapeutics and allowed escape from the chemotherapy-induced spindle assembly checkpoint. In support of these findings, direct comparison of DNA cross-linking and antimetabolic chemotherapeutics in primary FANCA^{-/-} cells revealed genomic instability originating through

*Corresponding author. Grzegorz Nalepa, Indiana University School of Medicine, Department of Pediatrics, Division of Pediatric Hematology-Oncology, Herman B Wells Center for Pediatric Research, 1044 W. Walnut Street, R4-421, Indianapolis, Indiana 46202, USA. Phone: 317.278.9846; Fax: 317.274.0138; gnalepa@iu.edu.
Z.A.S. and D.C. contributed equally to this work.

Publisher's Disclaimer: This is a PDF file of an unedited manuscript that has been accepted for publication. As a service to our customers we are providing this early version of the manuscript. The manuscript will undergo copyediting, typesetting, and review of the resulting proof before it is published in its final citable form. Please note that during the production process errors may be discovered which could affect the content, and all legal disclaimers that apply to the journal pertain.

This work was presented in part at the American Society of Hematology 55th Annual Meeting in New Orleans, LA, and at the American Society of Hematology 56th Annual Meeting in San Francisco, CA.

AUTHORSHIP

Z.A.S. and D.C. contributed equally to this work by performing experiments and editing the paper. E.S.P., Z.S., R.E., and Y.H. performed experiments. K.R. and W.S.G. obtained patient specimens and IRB approval. G.N. designed the study, supervised data analysis, and wrote the manuscript.

CONFLICT OF INTEREST DISCLOSURE

The authors declare that no conflicts of interest exist.

divergent cell cycle checkpoint aberrations. Our data indicate that the FA/BRCA signaling functions as an *in vivo* gatekeeper of genomic integrity throughout interphase and mitosis, which may have implications for future targeted therapies in FA and FA-deficient cancers.

INTRODUCTION

Fanconi anemia (FA/BRCA) pathway is an intricate plexus of at least 17 proteins that maintain genomic stability, control growth and development, and prevent cancer. Bi-allelic germline disruption of any FA gene causes Fanconi anemia (FA), a genetic disorder characterized by developmental abnormalities, bone marrow failure (BMF), myelodysplasia and high risk of cancer, particularly acute myeloid leukemia (AML)^{1–5}. Heterozygous inborn mutations in the BRCA branch of FA network increase risk of breast and ovarian cancers as well as other tumors^{5–9}, and somatic mutations of FA/BRCA genes occur in malignancies in non-Fanconi patients^{10–13}. Thus, disruption of FA/BRCA signaling promotes malignancies in the inherited genetic syndromes and in the general population.

The FA/BRCA pathway prevents cancer by protecting genome integrity. In interphase, DNA damage response (DDR) initiates the assembly of the multi-protein FA complex at damage sites to arrest the cell cycle as the cascade of effectors repairs the lesions^{1,5}. These compartmentalized bursts of FA activity handle multiple genotoxic insults, from endogenous aldehydes^{14,15} to replication errors and mutagen exposure. Thus, the FA/BRCA network provides a crucial line of defense against interphase mutagenesis^{1,5}.

Less is known about the role of the FA/BRCA pathway during mitosis, but FA signaling has been recently implicated in the maintenance of normal centrosome count^{16–19}, spindle assembly checkpoint (SAC)^{17,20}, repair of anaphase bridges^{21,22} and execution of cytokinesis^{23–25}. Since chromosomal instability due to mitotic errors is a hallmark of cancer^{26,27} and a therapeutic target²⁸, these findings may have translational relevance. However, it is unknown whether these *ex vivo* observations are applicable to *in vivo* hematopoiesis.

Here, we present quantitative evidence that loss of FA signaling disrupts mitosis during *in vivo* hematopoiesis in humans and mice, and that both aberrant interphase and mitotic failure contribute to genomic instability due to FA deficiency. Super-resolution microscopy revealed that FANCA shuttles to the pericentriolar material at mitotic entry to regulate centrosome-associated spindle nucleation. We found that primary *FANCA*–/– cells escape chemotherapy-induced SAC to replicate despite genomic instability. Our cell-survival assays showed that FA-deficient cells are hypersensitive to taxol (an antimitotic chemotherapeutic). Sublethal taxol doses exacerbated genomic instability in *FA*–/– cells through mitotic errors while low-dose MMC activated the G2/M checkpoint and DNA breakage. Therefore, distinct classes of chemotherapeutics inflict unique damage patterns in *FA*–/– cells, which may have implications for future strategies against FA-deficient cancers. Together, our findings provide insights into complex mechanisms of genomic instability in FA.

METHODS

Cell culture

The primary patient fibroblast cells, *FANCA*^{-/-} (MNHN, RA885), and *FANCC*^{-/-} (WD-C1, homozygous for *FANCC*^{c.377_378delGA}), were received from Dr. Helmut Hanenberg (IU). MNHN cells harbor two *FANCA* mutations: c.3163C>T, and c.4124-4125delCA. Both *FANCA*-deficient lines have been published¹⁷. Most experiments were done using the MNHN cells unless otherwise noted. Fibroblasts and MEFs were cultured in DMEM containing 10% fetal bovine serum (FBS), 1% penicillin-streptomycin (pen-strep), and 1% sodium pyruvate in 37°C-5%CO₂-5%O₂ incubators to minimize oxidative damage. Primary human CD34+ cells (IU Simon Cancer Center Angio BioCore) were incubated at 37°C-5%CO₂-5%O₂ in IMDM with 20% FBS, 1% pen-strep, 100 ng/ml SCF, 100ng/ml TPO, and 100ng/ml FLT3.

Mice

All animal experiments were approved by the Institutional Animal Care and Use Committee (IACUC) at IU School of Medicine. *Fancc*^{-/-} mice²⁹ were a gift from Dr. D. Wade Clapp (IU).

RBC micronucleation assays

50 µls of blood were collected from the murine lateral tail vein into EDTA-coated collection tubes containing methanol (2 mls, pre-chilled at -80°C for >1hr) and stored in -80°C. Next, 10ml PBS was added, cells were pelleted at 600×g (5 minutes, 4°C). The supernatant was aspirated and RBCs were resuspended in residual methanol/PBS. 20 µl aliquots were transferred to flow tubes and incubated in the dark with 90 µls of FITC-conjugated anti-mouse CD71 (Biolegend)+1 mg/ml RNase A (Roche) first for 30 minutes at room temperature (RT) and then 30 minutes on ice. Propidium iodide staining (Invitrogen) at 1.25 µg/ml was followed by flow cytometry on a FACS Calibur machine (Becton-Dickinson). At least 500,000 events/sample were acquired. Hemavet 950FS (Drew Scientific) was used for blood counts.

Deconvolution and super-resolution microscopy

Cells grown on ultrafine glass coverslips (Fisher) were fixed with 4% paraformaldehyde/PBS for 15 minutes (RT), PBS-washed, permeabilized with 0.1% Triton X-100/PBS for 10 minutes, PBS-washed, blocked in 5% bovine serum albumin (BSA)/PBS or ImageIT SignalEnhancer (Life Technologies) for 1 hour, and then incubated in primary antibody in 1% BSA/PBS overnight (4°C) or 2 hours (RT). Antibodies are listed in Supplemental Information. Next, cells were PBS-washed and incubated with secondary antibodies (1:2000, 1% BSA/PBS) for 30 minutes (RT), PBS-washed, counterstained with Hoechst-33342 (Life Technologies) in PBS (1:10,000) for 10 minutes, washed and mounted in SlowFade Antifade (Life Technologies).

For deconvolution microscopy, image stacks (z-section distance: 0.2µm) were acquired on a Deltavision personalDx microscope (Applied Precision) with a CCD camera using 20×, 60× or 100× lenses, and deconvolved using Softworx. Super-resolution structured illumination

microscopy (SR-SIM) images were acquired on a Zeiss ELYRA PS.1 system with a CCD camera and 60×/100× lenses, and processed via SIM/channel-alignment algorithms (Zen-2011; Zeiss). Line-intensity profiles were quantified using Imaris (Bitplane). Z-sections shown on figures were exported using Imaris.

Images of FA patient marrow aspirates, marrow aspirates of patients diagnosed with immune-mediated aplastic anemia with negative chromosome breakage test results, marrow cytopsins and peripheral smears were obtained on Zeiss Axiolab microscope with Axiocam-105 color camera.

Cytokinesis-block micronucleus assays

Fibroblasts and MEFs grown on coverslips were treated with cytochalasin B (2µg/ml) for 24 hours followed by processing/imaging as above; anti-CENPA immunofluorescence visualized endogenous kinetochores. For drug treatments, cells were exposed to 1nM taxol or MMC for 9 days before cytochalasin B for 24 hrs. A micronucleus was defined based on the following criteria: (1) the diameter of the micronucleus must be less than ½ of the main nucleus and (2) nuclear boundary must be identified between the micronucleus and the nucleus. The presence of kinetochores was determined based on visualization of CENPA+ foci within the stack of z-sections spanning the entire micronucleus.

For CD34+ experiments, primary human CD34+ cells transduced with GFP-tagged lentiviral shRNA constructs were cultured for 5 days, sorted on a SORP Aria FACS system, attached to coverslips via cytopsin (450rpm, 7 minutes), and analyzed in immunofluorescence assays as above.

Mitotic spindle assembly assay

Culture plates with live fibroblasts on coverslips were removed from the 37°C incubator to replace growth medium with pre-chilled medium and kept in 4°C (1 hour). Next, the cold medium was replaced with pre-warmed medium (37°C), cells were returned to 37°C (15 seconds), and immediately fixed (4% paraformaldehyde/PBS). Upon staining with anti-pericentrin and anti-α-tubulin, cells were imaged via deconvolution microscopy. Imaris (Bitplane) was used to measure length of microtubules in z-sections and count centrosome-associated microtubules within stacks.

Statistics

Statistical analyses were performed using GraphPad Prism 6; p<0.05 was considered significant.

Study approval

Patients had been enrolled on the IRB-approved protocol at IU School of Medicine (IRB#1108006474). All animal experiments were approved by the Institutional Animal Care and Use Committee (IACUC) at IU School of Medicine.

RESULTS

In vivo error-prone mitosis during FA^{-/-} hematopoiesis

Mitotic failure was reported in FA cells *ex vivo*, and cytokinesis failure was documented in FA marrows^{17,23}. However, the *in vivo* evidence of abnormal early mitosis in hematopoietic cells of FA patients has been missing. To examine whether loss of FANCA (the gene most commonly disrupted in FA⁵) predisposes hematopoietic cells to erratic divisions *in vivo*, we quantified mitotic errors in marrow aspirates of two *FANCA*^{-/-} patients with pancytopenia but no MDS/AML. Consistent with the role of FANCA in cell division, we observed increased frequency of abnormal mitotic figures in *FANCA*^{-/-} marrows compared to marrow aspirates of patients diagnosed with immune-mediated aplastic anemia after excluding FA by negative chromosome breakage tests (Figure 1A, *p*=0.01). Lack of chromosome congression leading to lagging chromosomes in anaphase and micronucleation at mitotic exit reflects weakened SAC or merotelic attachment due to centrosome malfunction¹⁷. The DNA bridges in late mitosis may reflect impaired resolution of ultrafine anaphase bridges²¹. Interphase nuclear morphology in the erythroid lineage provided further evidence of *in vivo* mitotic abnormalities (Figure 1B–C). Erythroblast micronucleation (Figure 1B) suggests failure to segregate chromosomes into the daughter nuclei. Presence of bizarre erythroblasts with multilobed nuclei (Figure 1B) is consistent with impaired chromosome segregation due to erroneous SAC followed by cytokinesis failure^{17,23}. Binucleated erythroblasts (Figure 1B) reflect lack of cytokinesis after normal chromosome division²³. These results provide quantitative *in vivo* evidence that abnormal mitoses occur with increased frequency in the hematopoietic cells of *FANCA*^{-/-} patients before development of MDS/AML.

We next validated these findings in a different *in vivo* experimental system. We examined hematopoietic chromosomal instability in living *Fancc*^{-/-} mice using an *in vivo* erythrocyte micronucleation assay^{30,31}. This assay is based on the notion that genomically unstable orthochromatic erythroblasts fail to extrude micronuclei, producing micronucleated red blood cells (RBCs). Indeed, we observed micronucleated RBCs in FA patients' marrows (Figure 1C). These micronucleated RBCs are identified via flow cytometry as DNA-containing CD71⁺ RBCs (Figure 1D). 3-month old *Fancc*^{-/-} mice released almost three-fold more micronucleated mature RBCs into the peripheral blood compared to age-matched controls (Figure 1D, *p*<0.0001). Importantly, blood counts demonstrated no differences between the age-matched *wt* and *Fancc*^{-/-} mice (Supplemental Table 1). Thus, disruption of two different FA core genes (*FANCA* and *Fancc*) leads to chromosomal instability during *in vivo* hematopoiesis in humans and mice before the onset of clinically significant BMF, myelodysplasia or leukemia.

A combination of interphase and mitotic errors drives genomic instability in FA

Since BMF and hematopoietic malignancies are consistent clinical hallmarks of FA^{1,5}, we quantified the contribution of interphase and mitotic abnormalities to genomic instability in FANCA-deficient hematopoietic cells. A modified micronucleus assay (Figure 2A)³² allowed to determine the origin of multinucleation in primary human CD34⁺ hematopoietic cells transduced with an shRNA against *FANCA*¹⁷ compared to control CD34⁺ cells. We

validated the *FANCA* shRNA in human CD34+ cells (Figure 2B–C). Upon *FANCA* knockdown, CD34+ cells were immunostained for endogenous CENPA (a kinetochore marker³³) and imaged by deconvolution microscopy to classify cells based on the presence of CENPA+ foci. As described³², additional kinetochore-positive nuclei arise through whole-chromosome missegregation in mitosis, and supernumerary kinetochore-negative nuclei result from DNA fragmentation (Figure 2A). *FANCA*-knockdown CD34+ cells developed higher multinucleation due to both chromosome breakage ($p=0.0083$) and faulty chromosome segregation ($p=0.0001$) compared to control CD34+ cells (Figure 2D–E). We concluded that silencing *FANCA* impairs both interphase and mitotic genome maintenance in human hematopoietic cells.

To validate this finding in primary FA-deficient patient cells and eliminate the possibility of non-specific shRNA-induced phenotype³⁴, we pursued cytokinesis-block cytochrome assays³². Dividing cells are treated with cytochalasin B (a cytokinesis inhibitor) prior to CENPA immunofluorescence. Inhibition of cytokinesis generates binucleated cells upon error-free chromosome partition, and the presence of micronuclei indicates abnormal chromosome segregation during the last mitosis. Again, CENPA-positivity distinguishes mitotic-failure micronuclei from DNA-breakage micronuclei (Figure 3A)³⁵.

FANCA^{−/−} fibroblasts had increased frequency of both chromosome missegregation ($p=0.0391$) and chromosome breakage ($p=0.0218$) compared to isogenic gene-corrected cells (Figure 3B–C). Similarly, *Fancc*^{−/−} MEFs demonstrated an increased incidence of micronucleation resulting from both chromosome breakage ($p=0.0004$) and chromosome missegregation ($p=0.078$) compared to *wt* MEFs (Figure 3D–E). Thus, disruption of FA signaling impairs interphase and mitotic fidelity not only during hematopoiesis (Figure 2), but also in fibroblasts and MEFs (Figure 3). These findings suggest that multiple FA/BRCA proteins may play evolutionarily conserved roles in mitotic genome housekeeping.

FANCA regulates centrosome-mediated spindle microtubule assembly in early mitosis

We and others have reported defects in centrosome amplification in cells lacking the FA/BRCA pathway^{16–19}, but the impact of FA signaling on mitotic centrosome function *per se* has not been studied. At mitotic entry, maturing centrosomes nucleate microtubules to build the mitotic spindle³⁶. These microtubules undergo controlled rearrangements to properly capture kinetochores before anaphase begins³⁷. Since *FANCA* localizes to the mitotic apparatus^{16,17} and FA signaling is implicated in the SAC¹⁷, we wondered whether *FANCA* regulates the dynamic equilibrium of spindle microtubule assembly in early mitosis. We quantified the ability of primary patient-derived *FANCA*^{−/−} and *FANCA*⁺ fibroblasts to establish spindles in modified spindle assembly assays (Figure 4A)³⁸. Live cells were first placed at 4°C to destabilize microtubules (Figure 4B) and then given pre-warmed growth medium to stimulate spindle regrowth, fixed and analyzed via quantitative deconvolution microscopy. Prometaphase *FANCA*^{−/−} centrosomes demonstrated impaired spindle-nucleating ability evidenced by decreased number of microtubules emanating from each centrosome (Figure 4C–D, $p=0.0001$). The spindle microtubules nucleated by *FANCA*^{−/−} centrosomes were shorter (Figure 4E, $p=0.0001$) than microtubules assembled in gene-corrected cells. Importantly, *FANCA*^{−/−} cells containing supernumerary centrosomes^{16,17}

were excluded from the analysis. Therefore, FANCA is essential not only for the maintenance of centrosome number, but also for efficient mitotic spindle assembly. Super-resolution structured illumination microscopy (SR-SIM) revealed endogenous FANCA on mitotic centrosomes in close proximity of spindle microtubules (Figure 4F–G), consistent with the role of FANCA in spindle dynamics.

FANCA shuttles to the pericentriolar material during mitotic centrosome maturation

Multiple FA proteins, including FANCA (Figure 4F–G), localize to centrosomes and mitotic spindles^{16–18}. However, it is unknown whether FANCA association with centrosomes changes between interphase and mitosis, as expected of a *bona fide* regulator of mitotic centrosome/spindle function^{39,40}.

Centrosome maturation prepares centrosomes for mitosis through reorganization of the pericentriolar material (PCM). A phosphosignaling circuit of cyclin-dependent kinases (CDKs), polo-like kinase 1 (PLK1) and Aurora A⁴¹ recruits pericentrin³⁹ and γ -tubulin⁴⁰ to the PCM at mitotic entry to increase the spindle-nucleating centrosome activity⁴². Since FANCA regulates spindle assembly (Figure 4B–E), we wondered whether FANCA is recruited to the PCM of maturing centrosomes similar to these other centrosome-spindle regulators. To examine FANCA sub-centrosomal localization, we employed deconvolution and super-resolution microscopy, which allows visualization of centrosomes beyond the diffraction limit imposed by conventional microscopes^{43,44}. At mitotic entry, FANCA shuttled from centrioles towards the PCM and co-localized with pericentrin, γ -tubulin and the minus end of spindle microtubules until the mitotic exit (Figure 5A–B, Supplemental Figures 4–7). In interphase, FANCA returned to the mother centriole (Supplemental Figure 8). These observations were confirmed with multiple primary antibodies and imaging of *FANCA*–/– patient cells stably expressing GFP-FANCA.

To thoroughly analyze FANCA distribution within the PCM, we analyzed individual 84-nm-thin super-resolution sections of mitotic centrosomes. At the mid-centrosome level, we observed well-organized FANCA fibers extending through and beyond the pericentrin-decorated PCM network from centrioles towards microtubule nucleation sites (Figure 5B–C). This dynamic relocation of FANCA to the PCM during mitosis supports the newly discovered role of FANCA in spindle microtubule nucleation (Figure 4).

Loss of *FANCA* allows escape from SAC arrest and apoptosis

The FA/BRCA pathway repairs interphase DNA damage^{45,46} and participates in the spindle assembly checkpoint (SAC)¹⁷. To examine the fate of *FANCA*-deficient cells upon SAC activation, we employed time-lapse imaging of primary *FANCA*–/– and gene-corrected cells treated with taxol, a microtubule-stabilizing chemotherapeutic (Figure 6A). As described in other cells^{47,48}, *FANCA*-corrected, taxol-exposed cells entered prolonged prometaphase arrest followed by cell death without exiting mitosis. *FANCA*–/– cells were more likely to escape taxol-induced SAC arrest and generate multinucleated interphase-like cells ($p=0.0215$; Figure 6B–E). These findings validate the role of FANCA in the SAC and show that loss of *FANCA* facilitates the escape of chromosomally unstable cells from mitotic death caused by unsatisfied SAC⁴⁷.

***FANCA*^{-/-} cells are hypersensitive to taxol**

A significant fraction of multinucleated cells that escape taxol-induced arrest⁴⁹ or form upon failed mitosis^{50,51} is physiologically eliminated to prevent genomic instability^{26,52}. Complete SAC disruption causes chromosomal instability incompatible with cell survival⁵³. Thus, we hypothesized that loss of *FANCA* may render cells hypersensitive to taxol.

Since previous studies evaluating response of *FA*^{-/-} cells to anti-mitotic chemotherapeutics generated conflicting data^{16,54}, we performed rigorous dose-response experiments to thoroughly examine this concept. We found that two separate *FANCA*^{-/-} primary patient cell lines harboring different *FANCA* mutations are hypersensitive to taxol; stable *FANCA* expression rescued taxol hypersensitivity in both lines in two independent cell viability assays (Figure 6F–H, Supplemental Figures 7–8). Likewise, *FANCC*^{-/-} primary fibroblasts displayed taxol hypersensitivity compared to *FANCC*-corrected cells (Supplemental Figure 8C). As expected^{1,5}, *FANCA*^{-/-} and *FANCC*^{-/-} cells showed decreased survival upon exposure to the crosslinking agent mitomycin C (MMC) (Figure 6F–H; Supplemental Figures 2,9). These findings, together with previously published work¹⁶, indicate that loss of *FANCA* or *FANCC* is synthetically lethal with exposure to anti-mitotic chemotherapeutics.

Chemotherapy-exposed *FANCA*^{-/-} cells develop distinct patterns of genomic instability due to separate interphase and mitotic checkpoint abnormalities

Having established the hypersensitivity of *FA*^{-/-} cells to interphase DNA crosslinkers and anti-mitotic agents, we wanted to understand how loss of *FANCA* confers hypersensitivity to these separate classes of chemotherapeutics. Thus, we examined cell cycle and patterns of genomic instability in primary *FANCA*^{-/-} and gene-corrected cells at baseline (Supplemental Figure 10) and upon treatment with sublethal doses of MMC and taxol. We selected drug doses that decreased growth of *FANCA*^{-/-} cells compared to isogenic *FANCA*⁺ cells without fully arresting *FANCA*^{-/-} cells or inducing cell death evidenced by increased sub-G1 fraction on flow cytometry (Figure 7A and not shown).

Prolonged treatment with 1 nM MMC reduced growth of *FANCA*^{-/-} cells due to persistent activation of the G2/M checkpoint ($p=0.0376$) reflected by decreased DNA replication ($p<0.0001$) and decreased G1 fraction ($p=0.0029$) (Figure 7A–D). This observation is consistent with the exaggerated MMC-induced G2/M arrest of *FA* cells due to the DDR failure^{45,46}. In further support of this notion, exposure to low-dose MMC increased multinucleation due to DNA breakage ($p=0.0223$) but not chromosome missegregation (Figure 7E–G). Sublethal taxol exposure affected *FANCA*^{-/-} cells differently. Prolonged treatment with low-dose taxol (but not MMC) significantly decreased the mitotic fraction of *FANCA*^{-/-} cells compared to gene-corrected cells (Figure 7H–I, $p<0.0001$) consistent with impaired SAC (Figure 6). Furthermore, low-dose taxol increased multinucleation of *FANCA*^{-/-} patient cells ($p=0.002$) secondary to mitotic chromosome missegregation ($p<0.0001$) as well as chromosome breakage ($p=0.0059$) (Figure 7J–K). Interestingly, multinucleated cells continued to enter S-phase (Supplemental Figure 11)^{52,55}.

In summary, these results (i) provide evidence that both impaired DDR and error-prone mitosis contribute to chromosomal instability in *FANCA*^{-/-} cells *in vivo* and *ex vivo*, (ii)

offer insights into the role of FA pathway in the response to DNA-crosslinking agents and anti-mitotic chemotherapeutics, and (iii) open potential new inroads towards synthetic lethal chemotherapy against FA-deficient cancers.

DISCUSSION

Disrupted FA/BRCA signaling causes genomic instability and cancer. The FA/BRCA tumor suppressor network orchestrates interphase DDR and DNA replication^{1,5}. Multiple lines of evidence implicated FA/BRCA signaling in centrosome maintenance and mitotic checkpoints^{16–19,21,23}, but the *in vivo* importance of these findings is unknown. We found that both abnormal interphase and error-prone mitosis significantly contribute to the *in vivo* hematopoietic genomic instability in FA^{–/–} humans and mice, suggesting a role for the FA/BRCA network in genome surveillance throughout the cell cycle (Figure 7L).

FANCA^{–/–} patients' hematopoiesis is afflicted by mitotic errors. Lagging chromosomes due to an *in vivo* SAC impairment¹⁷ and persistent anaphase/telophase bridges^{21,22} occur with increased frequency in FANCA^{–/–} patients (Figure 1). In agreement with the work from the D'Andrea group²³, bi-nucleated hematopoietic cells (Figure 1) are signs of faulty cytokinesis. Increased chromosome missegregation during erythropoiesis in FANCA^{–/–} mice (Figure 1D–E) indicates that other FA/BRCA proteins are essential for *in vivo* high-fidelity chromosome partition in hematopoietic cells in an evolutionary conserved manner. The onset of FA-associated mitotic abnormalities precedes the MDS/AML (Figure 1; Supplemental Table 1), suggesting that impaired mitosis may contribute to carcinogenesis in FA. Indeed, FISH analysis detected chromosomally unstable clones in 15% of FA patients with morphologically normal marrows⁵⁶, and gross chromosomal instability is a hallmark of MDS/AML in FA⁵⁷. More research is needed to quantify the impact of haphazard mitosis on FA-associated myelodysplasia and cancer.

The irregular mitosis during FA^{–/–} hematopoiesis is a consistent but relatively rare event (Figures 1–2). Further, while multinucleated cells with centrosome clusters are easily seen in FA-deficient cancer cells¹⁷, multinucleation in FA^{–/–} primary cells is more subtle (Figures 2–3)¹⁷, perhaps because cancers cannot eliminate mis-dividing cells through backup checkpoints. Indeed, centrosome abnormalities induce TP53-dependent cell cycle arrest⁵¹ and apoptosis⁵⁰, and activation of TP53 contributes to BMF in FA⁵⁸. TP53 inactivation boosts hematopoiesis but promotes MDS/AML in FA⁵⁹, and AML with bizarre karyotype instability occurred in an FA patient with somatic loss of heterozygosity of the TP53-harboring region of chromosome 17⁶⁰. Thus, aneuploidy and centrosome disruption upon inactivation of the FA/BRCA signaling may trigger TP53-dependent checkpoints to limit the risk of leukemia at the cost of BMF.

The role of FANCA in mitosis is not clearly defined. Impaired FA signaling promotes accumulation of centrosomes due to DDR-induced centrosome over-replication^{18,19} and deregulated mitosis^{17,23}. Supernumerary centrosomes promote chromosomal instability through multiple mechanisms^{26,61}. We found that FANCA regulates centrosome-associated spindle assembly (Figure 4), and FANCA shuttles from centrioles to the PCM spindle attachment sites at mitotic entry (Figures 4–5). Dissecting FANCA-dependent mitotic

centrosome-microtubule-kinetochore interactions in more detail will help understand how FANCA regulates the SAC¹⁷. We hypothesize that functional and numerical centrosome abnormalities in FA-deficient cells may further promote chromosomal instability by promoting merotelic kinetochore attachment to spindle microtubules; this mechanism of genomic instability has been elucidated in non-FA cells acquiring supernumerary centrosomes^{61,62}. Interestingly, FANCA is phosphorylated by the NIMA-related kinase 2 (NEK2)¹⁶ and AKT kinase⁶³; FANCI and FANCD1 may regulate polo-like kinase 1 (PLK1)^{18,19}, which is essential for spindle function⁶⁴; and FANCC binds the key mitotic cyclin-dependent kinase 1 (CDK1)⁶⁵, which co-immunoprecipitates with the FA core complex⁶⁶. Moreover, loss of FANCA is synthetic lethal with PLK1 knockdown⁶⁷ and CDK inhibitors disrupt IR-induced formation of FANCD2 foci⁶⁸. Future work will examine these pathway connections to evaluate their translational relevance in cancer and FA.

We found that loss of FA signaling is synthetically lethal with taxol exposure, highlighting the role of FA-dependent SAC in cell survival. Kim *et al* observed hypersensitivity of *FANCA*-knockdown cells to nocodazole¹⁶. Taxol and nocodazole are mechanistically different⁶⁹: nocodazole disrupts spindle-kinetochore attachment, while taxol renders the attached microtubules unable to stretch the kinetochores. Since the FA pathway is essential for taxol- and nocodazole-induced SAC¹⁷, FANCA may regulate SAC by intra-kinetochore tension.

Of note, others have found that *FANCG/FANCC*-deficient pancreatic cancer cells exposed to taxol accumulate DNA at similar rate as gene-corrected cells in *in vitro* fluorescence assays⁵⁴, and concluded that FA^{-/-} cells are not hypersensitive to antimetotics. However, FA^{-/-} cells multinucleate (Figure 6)^{16,17} and replicate (Supplemental Figure 11) upon exposure to antimetotics, suggesting why cell growth assays quantify taxol response with better specificity than total DNA measurements. Interestingly, low-dose taxol promotes chromosome missegregation and DNA breaks in *FANCA*^{-/-} cells. Consistent with this notion, the Pellman group demonstrated that micronuclei produced by mitotic errors undergo excessive mutagenesis⁵² with secondary chromosome breakage⁵⁵ due to erratic replication. The micronucleus-associated chromosome breakage may be further exacerbated by failed DDR in *FANCA*^{-/-} micronuclei.

Micronucleation has been noted in FA for decades^{70,71}, but it was unclear whether it reflects interphase abnormalities or erratic mitoses. We addressed this question with quantitative high-resolution-imaging-based micronucleation assays validated in previous studies³². Given the key role of FA signaling in interphase^{1,5}, we have made effort to confirm that kinetochore-containing micronuclei are not produced simply by impaired DDR. Importantly, DNA-crosslinking agent (MMC) produced “DNA breakage” micronuclei but not “chromosome missegregation” micronuclei (Figure 7F–G), confirming the assay’s specificity and sensitivity in distinguishing interphase from mitotic errors. Thus, we concluded that genomic instability results from DNA breakage and chromosome missegregation in multiple FA^{-/-} hematopoietic and non-hematopoietic cell types (Figures 2–3). Based on these and other findings¹⁷, we propose that FANCA deficiency causes genomic instability through a dual mechanism of impaired interphase DDR/replication and defective mitosis⁷² (Figure 7L). This model explains the FA-associated patterns of genetic

instability and hypersensitivity to both DNA-crosslinkers and antimetotics. Interphase errors exacerbate mitotic abnormalities and mitotic failure promotes interphase mutagenesis. Chromatid remnants generated through impaired DDR or replication are randomly segregated in mitosis. Defective midbody constriction²⁵ and cytokinesis²³ may shatter lagging chromosomes resulting from impaired SAC^{17,73} and break unresolved anaphase bridges^{21,22}. After mitotic exit, cells may attempt to repair splintered DNA through chromothripsis, the mutagenic process of randomly reconnecting chromosome fragments via non-homologous end joining (NHEJ)^{74–76}. Since FA^{–/–} cells favor error-prone NHEJ over homologous recombination⁷⁷, chromothripsis may have a particularly detrimental impact on genomic stability upon loss of the FA/BRCA network.

Our observations unveil the translational importance of mitotic defects caused by loss of FA/BRCA signaling. Somatic disruption of FA/BRCA genes occurs in malignancies in non-FA patients, including leukemia^{12,13,78,79}, cervical¹⁰, ovarian^{11,80,81}, breast⁸², bladder⁸³ and lung cancers⁸⁴. Our analysis of the COSMIC⁸⁵ database revealed multiple cancer-associated *FANCA* and *FANCC*-inactivating mutations in non-FA patients (**Supplemental Figure 13**). Since FA^{–/–} cells are hypersensitive to antimetotics, future preclinical studies will determine whether targeting mitosis can be employed in FA-deficient cancers. This strategy may complement other evidence-driven precision medicine efforts against FA^{–/–} cancers, such as targeting PARP-dependent DNA repair pathways^{86–88}, DNA damage kinases⁸⁹ and selective use of crosslinkers^{11,68}.

Supplementary Material

Refer to Web version on PubMed Central for supplementary material.

ACKNOWLEDGEMENTS

We are grateful to FA patients and families who generously provided cells used in this study. Primary FA patient fibroblasts were a kind gift of Drs. Helmut Hanenberg and D. Wade Clapp (IU). *Fancc*^{–/–} mice were a generous gift of Dr. D. Wade Clapp (IU). GN is supported by the NIH K12 Indiana Pediatric Scientist Award, by the Barth Syndrome/Bone Marrow Failure Research Fund at Riley Children's Foundation, and by the Heroes Foundation. DC was supported in part by Grant # UL1TR001108 (A. Shekhar, PI) from the NIH, National Center for Advancing Translational Sciences, Clinical and Translational Science Award, and T32 HL007910 "Basic Science Studies on Gene Therapy of Blood Diseases" grant. ESP was supported by T32 Pediatric Clinical Pharmacology Fellowship (NIH: 5 T32 HD69047-2) and T32 HL007910 "Basic Science Studies on Gene Therapy of Blood Diseases" grants.

REFERENCES

1. Kottmann MC, Smogorzewska A. Fanconi anaemia and the repair of Watson and Crick DNA crosslinks. *Nature*. 2013; 493(7432):356–363. [PubMed: 23325218]
2. Rosenberg PS, Alter BP, Ebell W. Cancer risks in Fanconi anemia: findings from the German Fanconi Anemia Registry. *Haematologica*. 2008; 93(4):511–517. [PubMed: 18322251]
3. Alter BP, Giri N, Savage SA, et al. Malignancies and survival patterns in the National Cancer Institute inherited bone marrow failure syndromes cohort study. *Br J Haematol*. 2010; 150(2):179–188. [PubMed: 20507306]
4. Alter BP. Fanconi anemia and the development of leukemia. *Best Pract Res Clin Haematol*. 2014; 27(3–4):214–221. [PubMed: 25455269]
5. D'Andrea AD. Susceptibility pathways in Fanconi's anemia and breast cancer. *N Engl J Med*. 2010; 362(20):1909–1919. [PubMed: 20484397]

6. Howlett NG, Taniguchi T, Olson S, et al. Biallelic inactivation of BRCA2 in Fanconi anemia. *Science*. 2002; 297(5581):606–609. [PubMed: 12065746]
7. Sawyer SL, Tian L, Kahkonen M, et al. Biallelic mutations in BRCA1 cause a new Fanconi anemia subtype. *Cancer Discov*. 2015; 5(2):135–142. [PubMed: 25472942]
8. Jones S, Hruban RH, Kamiyama M, et al. Exomic sequencing identifies PALB2 as a pancreatic cancer susceptibility gene. *Science*. 2009; 324(5924):5217.
9. Seal S, Thompson D, Renwick A, et al. Truncating mutations in the Fanconi anemia J gene BRIP1 are low-penetrance breast cancer susceptibility alleles. *Nat Genet*. 2006; 38(11):1239–1241. [PubMed: 17033622]
10. Narayan G, Arias-Pulido H, Nandula SV, et al. Promoter hypermethylation of FANCF: disruption of Fanconi Anemia-BRCA pathway in cervical cancer. *Cancer Res*. 2004; 64(9):2994–2997. [PubMed: 15126331]
11. Taniguchi T, Tischkowitz M, Ameziane N, et al. Disruption of the Fanconi anemia-BRCA pathway in cisplatin-sensitive ovarian tumors. *Nat Med*. 2003; 9(5):568–574. [PubMed: 12692539]
12. Tischkowitz M, Ameziane N, Waisfisz Q, et al. Bi-allelic silencing of the Fanconi anaemia gene FANCF in acute myeloid leukaemia. *Br J Haematol*. 2003; 123(3):469–471. [PubMed: 14617007]
13. Tischkowitz MD, Morgan NV, Grimwade D, et al. Deletion and reduced expression of the Fanconi anemia FANCA gene in sporadic acute myeloid leukemia. *Leukemia*. 2004; 18(3):420–425. [PubMed: 14749703]
14. Langevin F, Crossan GP, Rosado IV, Arends MJ, Patel KJ. Fancd2 counteracts the toxic effects of naturally produced aldehydes in mice. *Nature*. 2011; 475(7354):53–58. [PubMed: 21734703]
15. Garaycochea JI, Crossan GP, Langevin F, Daly M, Arends MJ, Patel KJ. Genotoxic consequences of endogenous aldehydes on mouse haematopoietic stem cell function. *Nature*. 2012; 489(7417):571–575. [PubMed: 22922648]
16. Kim S, Hwang SK, Lee M, et al. Fanconi anemia complementation group A (FANCA) localizes to centrosomes and functions in the maintenance of centrosome integrity. *Int J Biochem Cell Biol*. 2013; 45(9):1953–1961. [PubMed: 23806870]
17. Nalepa G, Enzor R, Sun Z, et al. Fanconi anemia signaling network regulates the spindle assembly checkpoint. *J Clin Invest*. 2013; 123(9):3839–3847. [PubMed: 23934222]
18. Zou J, Tian F, Li J, et al. FancJ regulates interstrand crosslinker induced centrosome amplification through the activation of polo-like kinase 1. *Biol Open*. 2013; 2(10):1022–1031. [PubMed: 24167712]
19. Zou J, Zhang D, Qin G, Chen X, Wang H, Zhang D. BRCA1 and FancJ cooperatively promote interstrand crosslinker induced centrosome amplification through the activation of polo-like kinase 1. *Cell Cycle*. 2014; 13(23):3685–3697. [PubMed: 25483079]
20. London N, Biggins S. Signalling dynamics in the spindle checkpoint response. *Nat Rev Mol Cell Biol*. 2014; 15(11):736–747. [PubMed: 25303117]
21. Naim V, Rosselli F. The FANC pathway and BLM collaborate during mitosis to prevent micronucleation and chromosome abnormalities. *Nat Cell Biol*. 2009; 11(6):761–768. [PubMed: 19465921]
22. Chan KL, Palmai-Pallag T, Ying S, Hickson ID. Replication stress induces sister-chromatid bridging at fragile site loci in mitosis. *Nat Cell Biol*. 2009; 11(6):753–760. [PubMed: 19465922]
23. Vinciguerra P, Godinho SA, Parmar K, Pellman D, D'Andrea AD. Cytokinesis failure occurs in Fanconi anemia pathway-deficient murine and human bone marrow hematopoietic cells. *J Clin Invest*. 2010; 120(11):3834–3842. [PubMed: 20921626]
24. Daniels MJ, Wang Y, Lee M, Venkitaraman AR. Abnormal cytokinesis in cells deficient in the breast cancer susceptibility protein BRCA2. *Science*. 2004; 306(5697):876–879. [PubMed: 15375219]
25. Mondal G, Rowley M, Guidugli L, Wu J, Pankratz VS, Couch FJ. BRCA2 localization to the midbody by filamin A regulates cep55 signaling and completion of cytokinesis. *Dev Cell*. 2012; 23(1):137–152. [PubMed: 22771033]
26. Gordon DJ, Resio B, Pellman D. Causes and consequences of aneuploidy in cancer. *Nat Rev Genet*. 2012; 13(3):189–203. [PubMed: 22269907]

27. Hanahan D, Weinberg RA. Hallmarks of cancer: the next generation. *Cell*. 2011; 144(5):646–674. [PubMed: 21376230]
28. Bakhoun SF, Compton DA. Chromosomal instability and cancer: a complex relationship with therapeutic potential. *J Clin Invest*. 2012; 122(4):1138–1143. [PubMed: 22466654]
29. Chen M, Tomkins DJ, Auerbach W, et al. Inactivation of Fac in mice produces inducible chromosomal instability and reduced fertility reminiscent of Fanconi anaemia. *Nat Genet*. 1996; 12(4):448–451. [PubMed: 8630504]
30. Cammerer Z, Schumacher MM, Kirsch-Volders M, Suter W, Elhajouji A. Flow cytometry peripheral blood micronucleus test in vivo: determination of potential thresholds for aneuploidy induced by spindle poisons. *Environ Mol Mutagen*. 2010; 51(4):278–284. [PubMed: 19950395]
31. Balmus G, Karp NA, Ng BL, Jackson SP, Adams DJ, McIntyre RE. A high-throughput in vivo micronucleus assay for genome instability screening in mice. *Nat Protoc*. 2015; 10(1):205–215. [PubMed: 25551665]
32. Fenech M. Cytokinesis-block micronucleus cytome assay. *Nat Protoc*. 2007; 2(5):1084–1104. [PubMed: 17546000]
33. Palmer DK, O'Day K, Trong HL, Charbonneau H, Margolis RL. Purification of the centromere-specific protein CENP-A and demonstration that it is a distinctive histone. *Proc Natl Acad Sci U S A*. 1991; 88(9):3734–3738. [PubMed: 2023923]
34. Sigoillot FD, Lyman S, Huckins JF, et al. A bioinformatics method identifies prominent off-targeted transcripts in RNAi screens. *Nat Methods*. 2012; 9(4):363–366. [PubMed: 22343343]
35. Schuler M, Rupa DS, Eastmond DA. A critical evaluation of centromeric labeling to distinguish micronuclei induced by chromosomal loss and breakage in vitro. *Mutat Res*. 1997; 392(1–2):81–95. [PubMed: 9269333]
36. Brownlee CW, Rogers GC. Show me your license, please: deregulation of centriole duplication mechanisms that promote amplification. *Cell Mol Life Sci*. 2013; 70(6):1021–1034. [PubMed: 22892665]
37. Godek KM, Kabeche L, Compton DA. Regulation of kinetochore-microtubule attachments through homeostatic control during mitosis. *Nat Rev Mol Cell Biol*. 2015; 16(1):57–64. [PubMed: 25466864]
38. O'Rourke BP, Gomez-Ferreria MA, Berk RH, et al. Cep192 controls the balance of centrosome and non-centrosomal microtubules during interphase. *PLoS One*. 2014; 9(6):e101001. [PubMed: 24971877]
39. Lee K, Rhee K. PLK1 phosphorylation of pericentrin initiates centrosome maturation at the onset of mitosis. *J Cell Biol*. 2011; 195(7):1093–1101. [PubMed: 22184200]
40. Sdelci S, Schutz M, Pinyol R, et al. Nek9 phosphorylation of NEDD1/GCP-WD contributes to Plk1 control of gamma-tubulin recruitment to the mitotic centrosome. *Curr Biol*. 2012; 22(16):1516–1523. [PubMed: 22818914]
41. Joukov V, Walter JC, De Nicolo A. The Cep192-organized aurora A-Plk1 cascade is essential for centrosome cycle and bipolar spindle assembly. *Mol Cell*. 2014; 55(4):578–591. [PubMed: 25042804]
42. Zimmerman WC, Sillibourne J, Rosa J, Doxsey SJ. Mitosis-specific anchoring of gamma tubulin complexes by pericentrin controls spindle organization and mitotic entry. *Mol Biol Cell*. 2004; 15(8):3642–3657. [PubMed: 15146056]
43. Lawo S, Hasegan M, Gupta GD, Pelletier L. Subdiffraction imaging of centrosomes reveals higher-order organizational features of pericentriolar material. *Nat Cell Biol*. 2012; 14(11):1148–1158. [PubMed: 23086237]
44. Mennella V, Agard DA, Huang B, Pelletier L. Amorphous no more: subdiffraction view of the pericentriolar material architecture. *Trends Cell Biol*. 2014; 24(3):188–197. [PubMed: 24268653]
45. Chandra S, Levran O, Jurickova I, et al. A rapid method for retrovirus-mediated identification of complementation groups in Fanconi anemia patients. *Mol Ther*. 2005; 12(5):976–984. [PubMed: 16084127]
46. Heinrich MC, Hoatlin ME, Zigler AJ, et al. DNA cross-linker-induced G2/M arrest in group C Fanconi anemia lymphoblasts reflects normal checkpoint function. *Blood*. 1998; 91(1):275–287. [PubMed: 9414295]

47. Woods CM, Zhu J, McQueney PA, Bollag D, Lazarides E. Taxol-induced mitotic block triggers rapid onset of a p53-independent apoptotic pathway. *Mol Med*. 1995; 1(5):506–526. [PubMed: 8529117]
48. Jordan MA, Wendell K, Gardiner S, Derry WB, Copp H, Wilson L. Mitotic block induced in HeLa cells by low concentrations of paclitaxel (Taxol) results in abnormal mitotic exit and apoptotic cell death. *Cancer Res*. 1996; 56(4):816–825. [PubMed: 8631019]
49. Torres K, Horwitz SB. Mechanisms of Taxol-induced cell death are concentration dependent. *Cancer Res*. 1998; 58(16):3620–3626. [PubMed: 9721870]
50. Cuomo ME, Knebel A, Morrice N, Paterson H, Cohen P, Mitnacht S. p53-Driven apoptosis limits centrosome amplification and genomic instability downstream of NPM1 phosphorylation. *Nat Cell Biol*. 2008; 10(6):723–730. [PubMed: 18454140]
51. Mikule K, Delaval B, Kaldis P, Jurczyk A, Hergert P, Doxsey S. Loss of centrosome integrity induces p38-p53-p21-dependent G1-S arrest. *Nat Cell Biol*. 2007; 9(2):160–170. [PubMed: 17330329]
52. Crasta K, Ganem NJ, Dagher R, et al. DNA breaks and chromosome pulverization from errors in mitosis. *Nature*. 2012; 482(7383):53–58. [PubMed: 22258507]
53. Dobles M, Liberal V, Scott ML, Benezra R, Sorger PK. Chromosome missegregation and apoptosis in mice lacking the mitotic checkpoint protein Mad2. *Cell*. 2000; 101(6):635–645. [PubMed: 10892650]
54. van der Heijden MS, Brody JR, Dezentje DA, et al. In vivo therapeutic responses contingent on Fanconi anemia/BRCA2 status of the tumor. *Clin Cancer Res*. 2005; 11(20):7508–7515. [PubMed: 16243825]
55. Zhang CZ, Spektor A, Cornils H, et al. Chromothripsis from DNA damage in micronuclei. *Nature*. 2015; 522(7555):179–184. [PubMed: 26017310]
56. Mehta PA, Harris RE, Davies SM, et al. Numerical chromosomal changes and risk of development of myelodysplastic syndrome--acute myeloid leukemia in patients with Fanconi anemia. *Cancer Genet Cytogenet*. 2010; 203(2):180–186. [PubMed: 21156231]
57. Quentin S, Cucchini W, Ceccaldi R, et al. Myelodysplasia and leukemia of Fanconi anemia are associated with a specific pattern of genomic abnormalities that includes cryptic RUNX1/AML1 lesions. *Blood*. 2011; 117(15):e161–e170. [PubMed: 21325596]
58. Ceccaldi R, Parmar K, Mouly E, et al. Bone marrow failure in Fanconi anemia is triggered by an exacerbated p53/p21 DNA damage response that impairs hematopoietic stem and progenitor cells. *Cell Stem Cell*. 2012; 11(1):36–49. [PubMed: 22683204]
59. Ceccaldi R, Briot D, Larghero J, et al. Spontaneous abrogation of the G(2)DNA damage checkpoint has clinical benefits but promotes leukemogenesis in Fanconi anemia patients. *J Clin Invest*. 2011; 121(1):184–194. [PubMed: 21183791]
60. Woo HI, Kim HJ, Lee SH, Yoo KH, Koo HH, Kim SH. Acute myeloid leukemia with complex hypodiploidy and loss of heterozygosity of 17p in a boy with Fanconi anemia. *Ann Clin Lab Sci*. 2011; 41(1):66–70. [PubMed: 21325258]
61. Ganem NJ, Godinho SA, Pellman D. A mechanism linking extra centrosomes to chromosomal instability. *Nature*. 2009; 460(7252):278–282. [PubMed: 19506557]
62. Nam HJ, Naylor RM, van Deursen JM. Centrosome dynamics as a source of chromosomal instability. *Trends Cell Biol*. 2015; 25(2):65–73. [PubMed: 25455111]
63. Otsuki T, Nagashima T, Komatsu N, et al. Phosphorylation of Fanconi anemia protein, FANCA, is regulated by Akt kinase. *Biochem Biophys Res Commun*. 2002; 291(3):628–634. [PubMed: 11855836]
64. Sumara I, Gimenez-Abian JF, Gerlich D, et al. Roles of polo-like kinase 1 in the assembly of functional mitotic spindles. *Curr Biol*. 2004; 14(19):1712–1722. [PubMed: 15458642]
65. Kupfer GM, Yamashita T, Naf D, Suliman A, Asano S, D'Andrea AD. The Fanconi anemia polypeptide, FAC, binds to the cyclin-dependent kinase, cdc2. *Blood*. 1997; 90(3):1047–1054. [PubMed: 9242535]
66. Thomashevski A, High AA, Drozd M, et al. The Fanconi anemia core complex forms four complexes of different sizes in different subcellular compartments. *J Biol Chem*. 2004; 279(25):26201–26209. [PubMed: 15082718]

67. Kennedy RD, Chen CC, Stuckert P, et al. Fanconi anemia pathway-deficient tumor cells are hypersensitive to inhibition of ataxia telangiectasia mutated. *J Clin Invest.* 2007; 117(5):1440–1449. [PubMed: 17431503]
68. Jacquemont C, Simon JA, D'Andrea AD, Taniguchi T. Non-specific chemical inhibition of the Fanconi anemia pathway sensitizes cancer cells to cisplatin. *Mol Cancer.* 2012; 11:26. [PubMed: 22537224]
69. Maresca TJ, Salmon ED. Welcome to a new kind of tension: translating kinetochore mechanics into a wait-anaphase signal. *J Cell Sci.* 2010; 123(Pt 6):825–835. [PubMed: 20200228]
70. Barton JC, Parmley RT, Carroll AJ, et al. Preleukemia in Fanconi's anemia: hematopoietic cell multinuclearity, membrane duplication, and dysgranulogenesis. *J Submicrosc Cytol.* 1987; 19(2): 355–364. [PubMed: 3599130]
71. Willingale-Theune J, Schweiger M, Hirsch-Kauffmann M, Meek AE, Paulin-Levasseur M, Traub P. Ultrastructure of Fanconi anemia fibroblasts. *J Cell Sci.* 1989; 93(Pt 4):651–665. [PubMed: 2691519]
72. Nalepa G, Clapp DW. Fanconi anemia and the cell cycle: new perspectives on aneuploidy. *F1000Prime Rep.* 2014; 6:23. [PubMed: 24765528]
73. Choi E, Park PG, Lee HO, et al. BRCA2 fine-tunes the spindle assembly checkpoint through reinforcement of BubR1 acetylation. *Dev Cell.* 2012; 22(2):295–308. [PubMed: 22340495]
74. Maher CA, Wilson RK. Chromothripsis and human disease: piecing together the shattering process. *Cell.* 2012; 148(1–2):29–32. [PubMed: 22265399]
75. Zhang CZ, Leibowitz ML, Pellman D. Chromothripsis and beyond: rapid genome evolution from complex chromosomal rearrangements. *Genes Dev.* 2013; 27(23):2513–2530. [PubMed: 24298051]
76. Forment JV, Kaidi A, Jackson SP. Chromothripsis and cancer: causes and consequences of chromosome shattering. *Nat Rev Cancer.* 2012; 12(10):663–670. [PubMed: 22972457]
77. Adamo A, Collis SJ, Adelman CA, et al. Preventing nonhomologous end joining suppresses DNA repair defects of Fanconi anemia. *Mol Cell.* 2010; 39(1):25–35. [PubMed: 20598602]
78. Hess CJ, Ameziane N, Schuurhuis GJ, et al. Hypermethylation of the FANCC and FANCL promoter regions in sporadic acute leukaemia. *Cell Oncol.* 2008; 30(4):299–306. [PubMed: 18607065]
79. Xie Y, de Winter JP, Waisfisz Q, et al. Aberrant Fanconi anaemia protein profiles in acute myeloid leukaemia cells. *Br J Haematol.* 2000; 111(4):1057–1064. [PubMed: 11167740]
80. Wang Z, Li M, Lu S, Zhang Y, Wang H. Promoter hypermethylation of FANCF plays an important role in the occurrence of ovarian cancer through disrupting Fanconi anemia-BRCA pathway. *Cancer Biol Ther.* 2006; 5(3):256–260. [PubMed: 16418574]
81. Olopade OI, Wei M. FANCF methylation contributes to chemoselectivity in ovarian cancer. *Cancer Cell.* 2003; 3(5):417–420. [PubMed: 12781358]
82. Wei M, Xu J, Dignam J, et al. Estrogen receptor alpha, BRCA1, and FANCF promoter methylation occur in distinct subsets of sporadic breast cancers. *Breast Cancer Res Treat.* 2008; 111(1):113–120. [PubMed: 17932744]
83. Neveling K, Kalb R, Florl AR, et al. Disruption of the FA/BRCA pathway in bladder cancer. *Cytogenet Genome Res.* 2007; 118(2–4):166–176. [PubMed: 18000367]
84. Marsit CJ, Liu M, Nelson HH, Posner M, Suzuki M, Kelsey KT. Inactivation of the Fanconi anemia/BRCA pathway in lung and oral cancers: implications for treatment and survival. *Oncogene.* 2004; 23(4):1000–1004. [PubMed: 14647419]
85. Forbes SA, Beare D, Gunasekaran P, et al. COSMIC: exploring the world's knowledge of somatic mutations in human cancer. *Nucleic Acids Res.* 2015; 43(Database issue):D805–D811. [PubMed: 25355519]
86. Ceccaldi R, Liu JC, Amunugama R, et al. Homologous-recombination-deficient tumours are dependent on Poltheta-mediated repair. *Nature.* 2015; 518(7538):258–262. [PubMed: 25642963]
87. Bryant HE, Schultz N, Thomas HD, et al. Specific killing of BRCA2-deficient tumours with inhibitors of poly(ADP-ribose) polymerase. *Nature.* 2005; 434(7035):913–917. [PubMed: 15829966]

88. Farmer H, McCabe N, Lord CJ, et al. Targeting the DNA repair defect in BRCA mutant cells as a therapeutic strategy. *Nature*. 2005; 434(7035):917–921. [PubMed: 15829967]
89. Chen CC, Kennedy RD, Sidi S, Look AT, D'Andrea A. CHK1 inhibition as a strategy for targeting Fanconi Anemia (FA) DNA repair pathway deficient tumors. *Mol Cancer*. 2009; 8:24. [PubMed: 19371427]

Author Manuscript

Author Manuscript

Author Manuscript

Author Manuscript

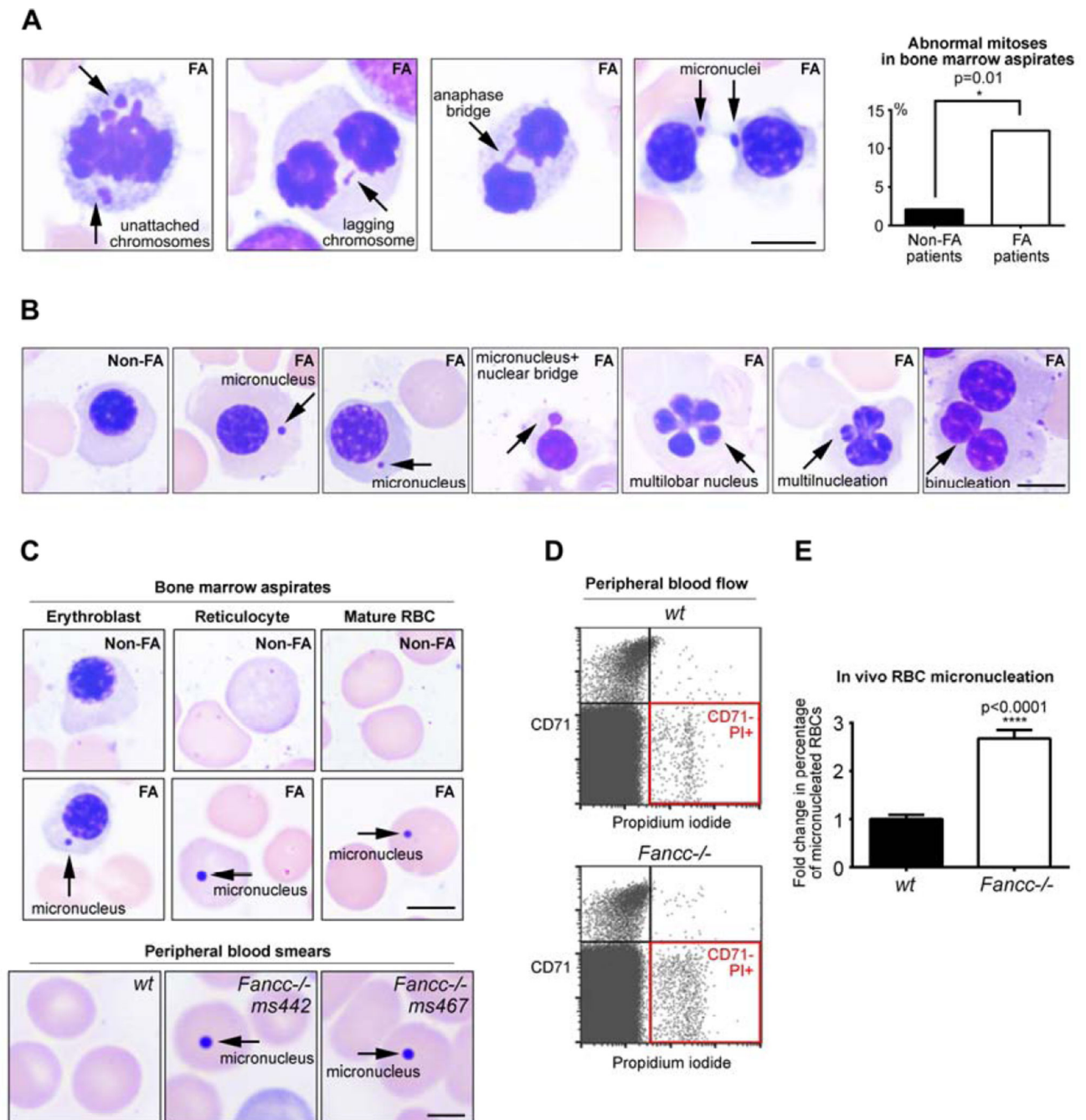


Figure 1. *In vivo* chromosomal instability and abnormal mitoses during human *FANCA*^{-/-} and murine *Fancc*^{-/-} hematopoiesis

(A) Representative abnormal mitoses in *FANCA*^{-/-} patient bone marrow aspirates. Quantification (upper right) represents data from 2 different FA patients and 2 non-FA patients (96 mitoses in non-FA and 73 mitoses in FA; Fisher's exact test). Scale bars: 5 μ m. (B) Examples of abnormal interphase nuclear morphology in *FANCA*^{-/-} patients' hematopoietic cells that have undergone aberrant mitoses compared to a normal non-FA interphase erythroblast. Scale bars: 5 μ m (C) Micronucleation of *FANCA*^{-/-} bone marrow

erythroblasts, reticulocytes and mature red blood cells (top) and *Fancc*^{-/-} murine RBCs in peripheral blood (bottom). Scale bars: 5 μ m (top); 2 μ m (bottom). **(D)** Increased frequency of CD71⁻, PI⁺ micronucleated mature RBCs in peripheral blood of 3-month-old *Fancc*^{-/-} mice. **(E)** Quantification of micronucleated RBCs identified by flow cytometry is shown as fold change relative to wild-type levels. Bars indicate mean \pm SEM; >10 age-matched mice/genotype from multiple independent experiments were analyzed using a student's t-test. All specimens were imaged with Zeiss AxioLab system equipped with an AxioCam 105 color camera.

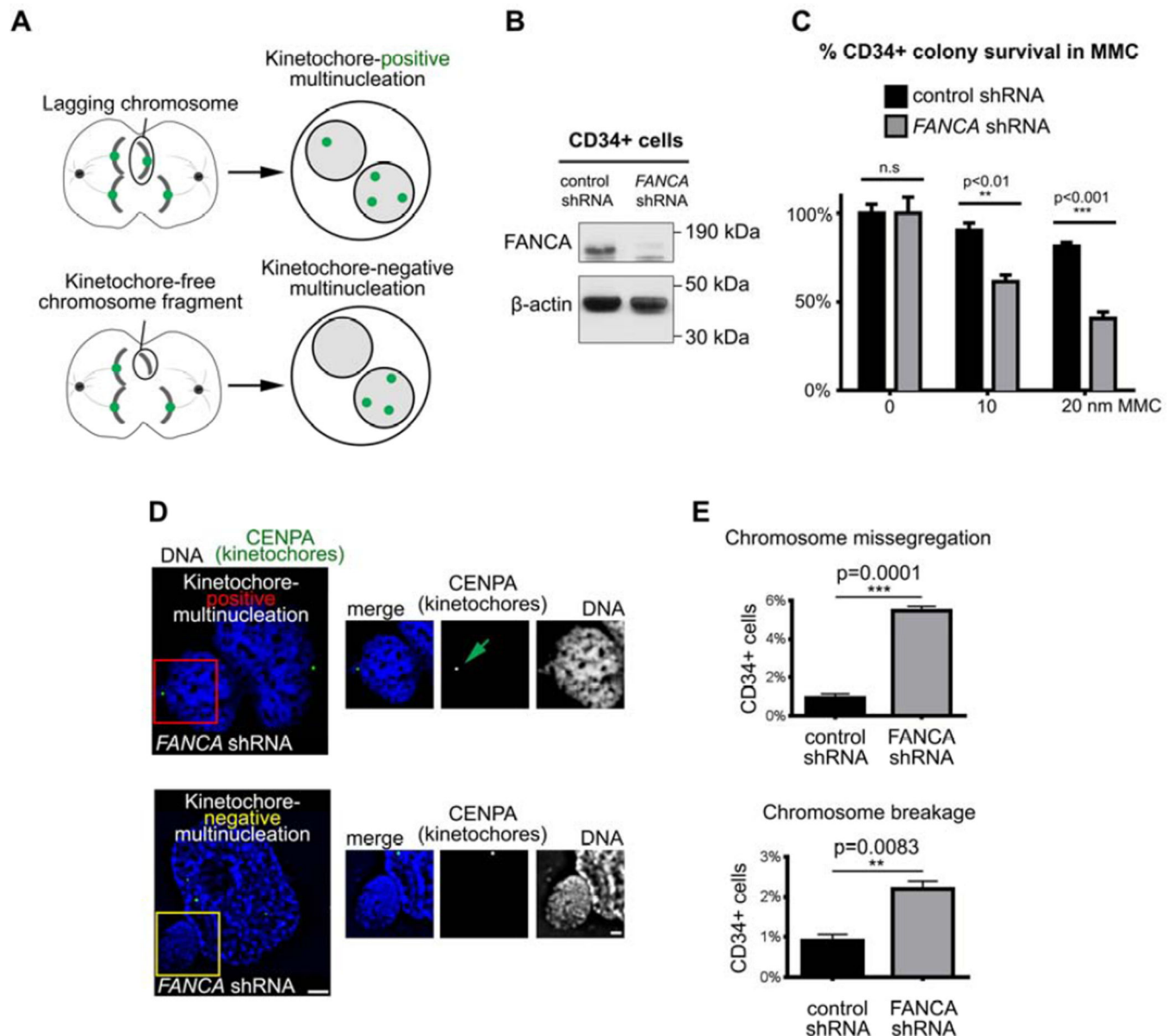


Figure 2. FANCA maintains genomic integrity during interphase and mitosis in primary human CD34+ cells

(A) Assay schematic. Kinetochore/centrosome immunofluorescence staining distinguishes multinucleation generated through whole-chromosome missegregation from multinucleation resulting from DNA breakage. (B) *FANCA* shRNA efficiently knocks down *FANCA* protein in primary human CD34+ cells. β -actin serves as loading control. (C) Functional validation of *FANCA* shRNA in primary human CD34+ cells. *FANCA* shRNA renders CD34+ cells hypersensitive to mitomycin C compared to CD34+ cells compared with control shRNA. Error bars represent mean \pm SEM and significance was determined using a two-way ANOVA with Sidak correction. (D) Representative images of multinucleation resulting from *FANCA* knockdown in human CD34+ cells. Regions of interests are marked in red or yellow and enlarged on the right. Green arrow points to a CENPA-positive centromere/

kinetochore within the supernumerary nucleus. Scale bars: 2 μ m (left) and 1 μ m (right) (**E**)
Quantification of multinucleation resulting from weakened SAC or chromosome breakage in control and FANCA-knockdown CD34+ cells. At least 500 cells per group were counted. Results were analyzed using a student's t-test and represented as mean \pm SEM.

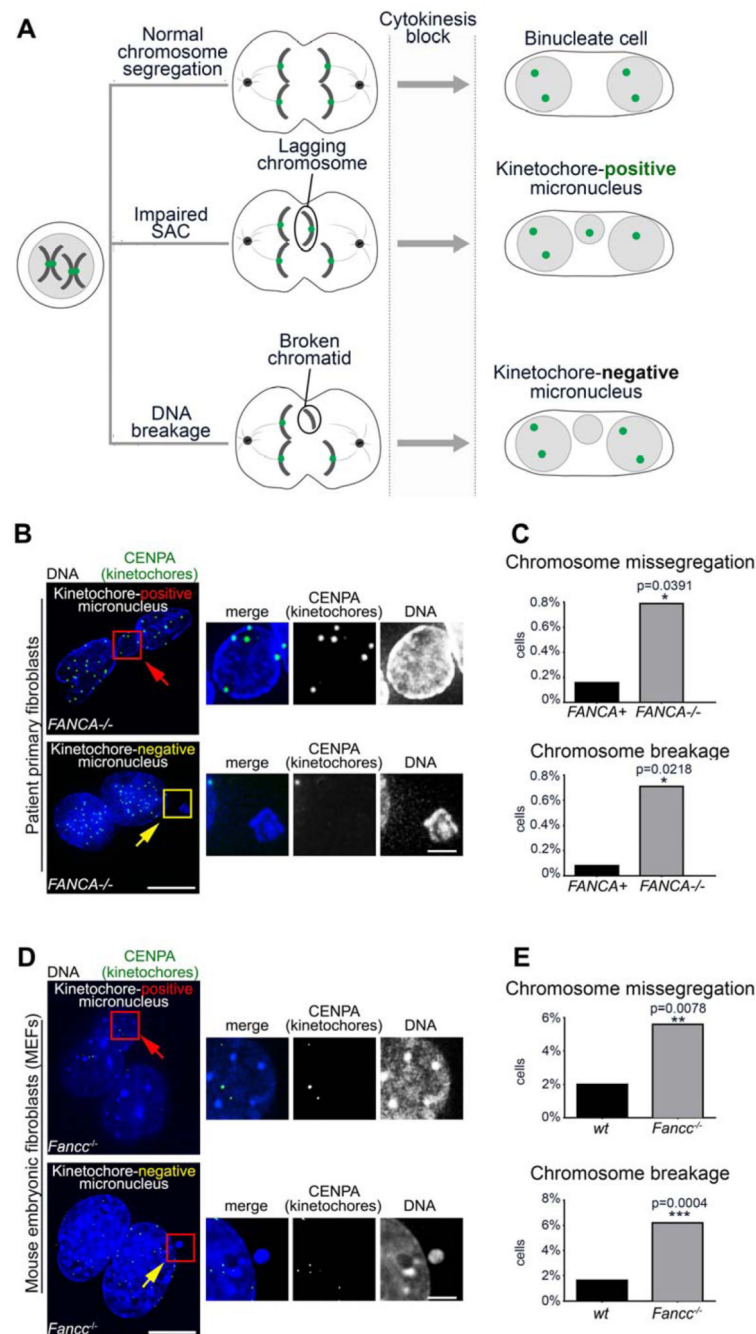


Figure 3. Micronucleation upon loss of FA signaling results from a combination of interphase and mitotic errors

(A) Schematic of cytokinesis-block micronucleus test that discriminates the origin of aneuploidy based on the presence or absence of kinetochores within micronuclei. (B) Representative images of micronuclei in *FANCA*^{-/-} primary patient fibroblasts. Scale bars: 10µm (left) and 2µm (right) (C) Quantification of micronuclei resulting from whole-chromosome missegregation versus chromosome breakage in primary *FANCA*^{-/-} and *FANCA*⁺ fibroblasts. Error bars represent mean \pm SEM. (D) Representative images of

micronuclei in *Fancc*^{-/-} MEFs. Scale bars: 10µm (left) and 2µm (right) (E) Quantification of micronucleation resulting from chromosome missegregation and chromosome breakage in *wt* and *Fancc*^{-/-} MEFs. At least 260 cells were counted per condition and significance was determined by student's t-test. Cells were imaged with deconvolution microscopy (Applied Precision personalDx) and deconvolved with Softworx imaging suite (10 iterations, ratio: conservative).

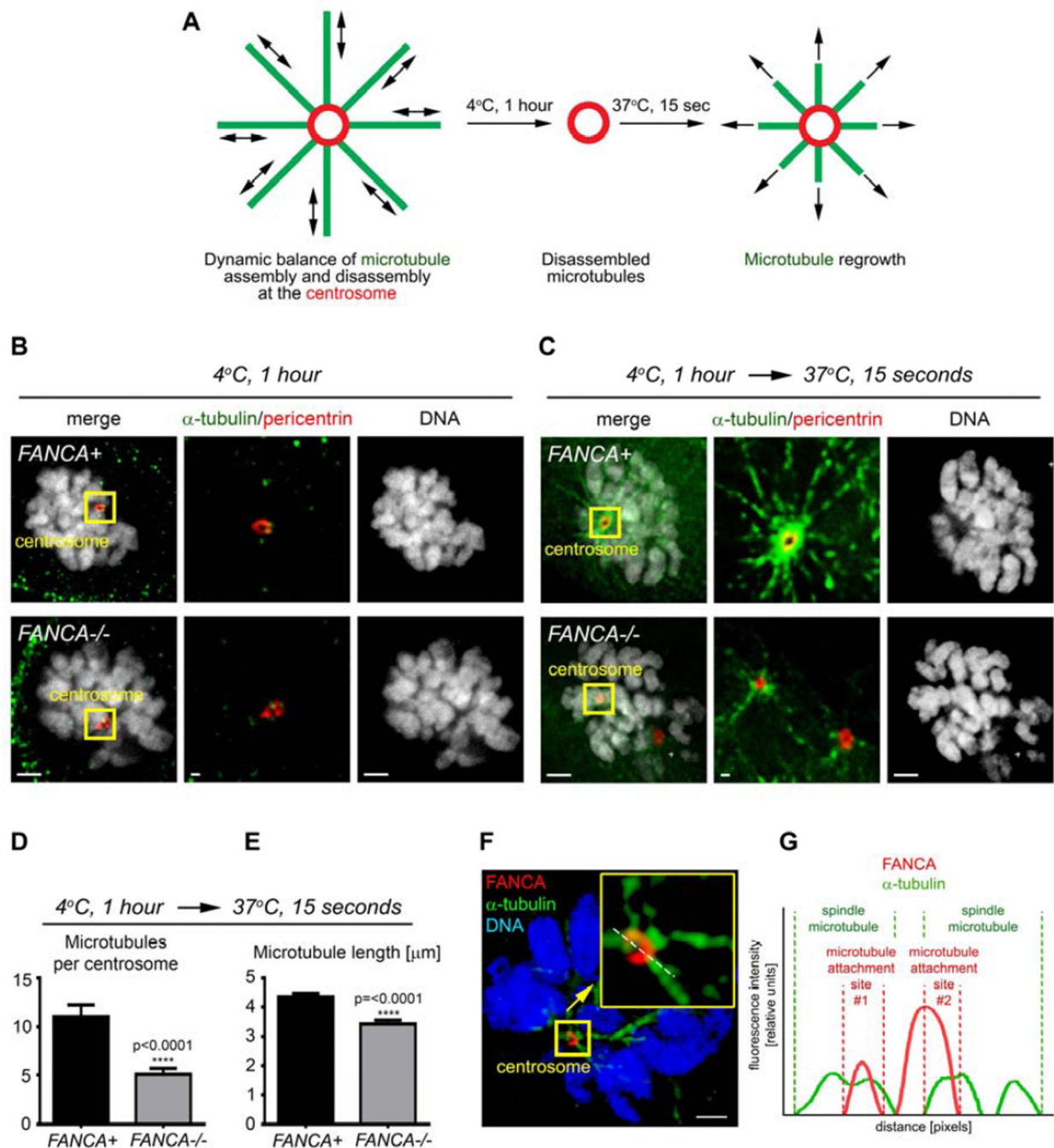


Figure 4. Loss of FANCA disrupts spindle microtubule assembly at prometaphase centrosomes
(A) Experiment design. Microtubules of living *FANCA*^{-/-} and *FANCA*⁺ cells were destabilized by cold treatment (4°C for 1 hour). Cells were then returned to 37°C to initiate microtubule reassembly and fixed with 4% paraformaldehyde 15 seconds later. **(B)** Cold treatment fully destabilizes microtubules in *FANCA*⁺ and *FANCA*^{-/-} prometaphase cells. **(C)** Representative images of mitotic spindle assembly in *FANCA*⁺ and *FANCA*^{-/-} prometaphase cells stained with anti- α -tubulin (green) and anti-pericentrin (red) antibodies. Images were captured with 60 \times lens on the Deltavision deconvolution microscope. Scale

bars: 2 μ m (left and right) and 500nm (region of interest showed in the center). **(D, E)** Quantification of spindle microtubules per centrosome **(D)** and the microtubule length (μ M) **(E)** in gene-corrected and *FANCA*^{-/-} cells treated as described in **(A)**. Data represents 2 independent experiments (n=130 microtubules/experiment), and error bars represent SEM. **(E)** Representative mitotic HeLa cell stained with anti-FANCA (red) and anti- α -tubulin (green) antibodies, imaged on an ELYRA PS.1 super-resolution microscope using SIM technology. Insert shows enlarged centrosome-containing region of interest. White line shows the line of fluorescence intensity profile. Scale bar: 2 μ m. Cells were imaged with deconvolution microscopy (Applied Precision personalDx) and deconvolved with Softworx imaging suite (10 iterations, ratio: conservative). **(F)** Fluorescence intensity profiles of FANCA (red) and α -tubulin (green) signal.

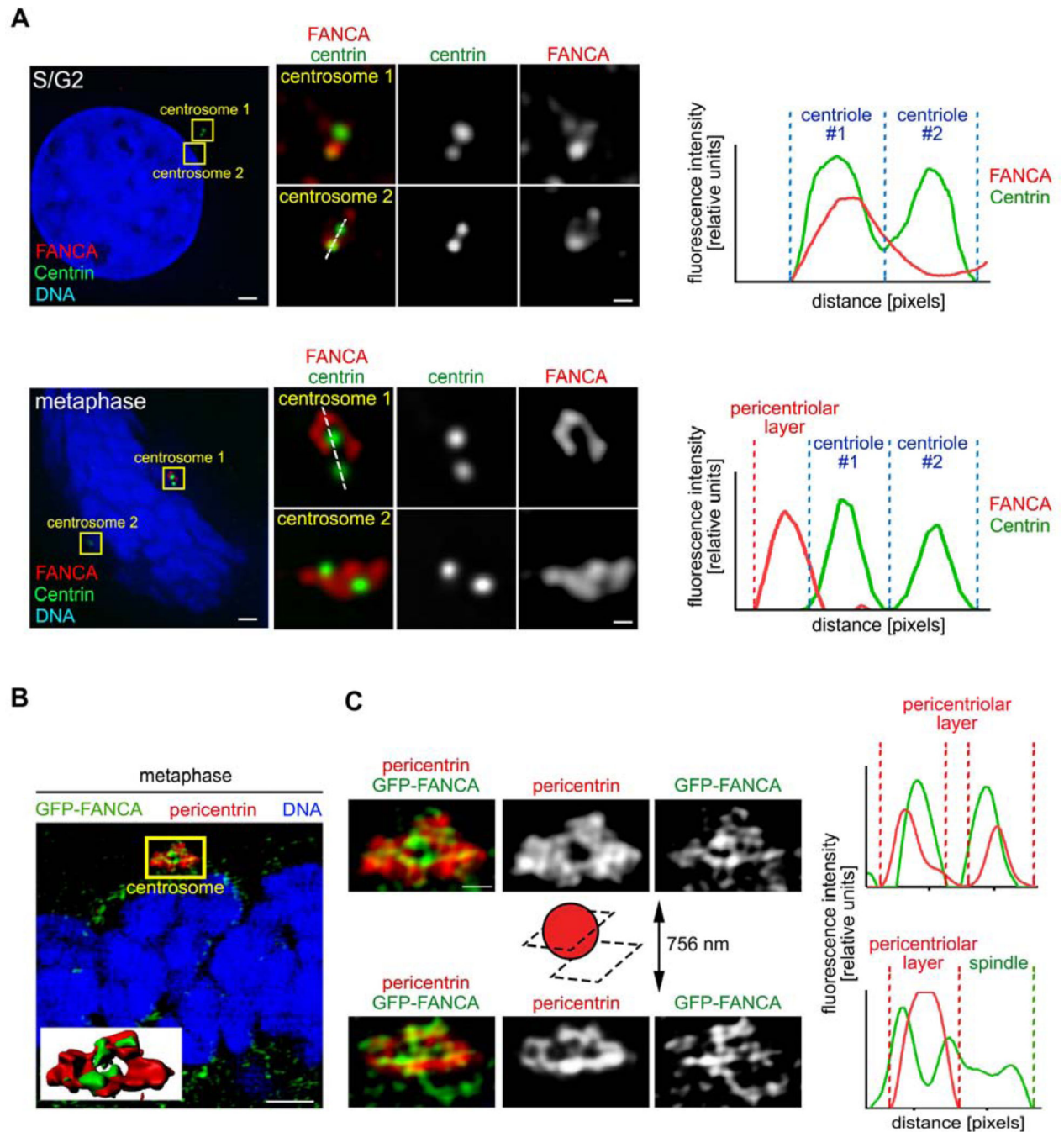


Figure 5. FANCA shuttles to the pericentriolar material during mitosis

(A) HeLa cells were immunostained with antibodies against endogenous FANCA (red) and centrin (green), imaged with deconvolution microscopy (Applied Precision personalDx) and deconvolved with Softworx imaging suite (10 iterations, ratio: conservative). Fluorescence intensity profiles demonstrate that FANCA colocalizes with centrin in interphase and migrates away from centrosomes at metaphase. Scale bars: 1.5 μ m (left) and 300 nm (right) (B) Representative super-resolution image of human fibroblast stably expressing GFP-FANCA and stained with antibody against the pericentriolar material marker (pericentrin). Inserted

3D rendering of the centrosome shows colocalization of GFP-FANCA and pericentrin. Scale bars: 2 μm . The yellow region of interest is magnified (**C**) to show FANCA fibers embedded within the PCM (centrosome cross-section) and extending towards the spindle (centrosome outer layer section). Fluorescence intensity profiles (right) of GFP-FANCA/pericentrin signal at PCM and spindle are shown on the right. Scale bar: 500 nm. SR-SIM images were acquired on Zeiss ELYRA PS.1 super-resolution microscopy system and exported using Imaris imaging suite.

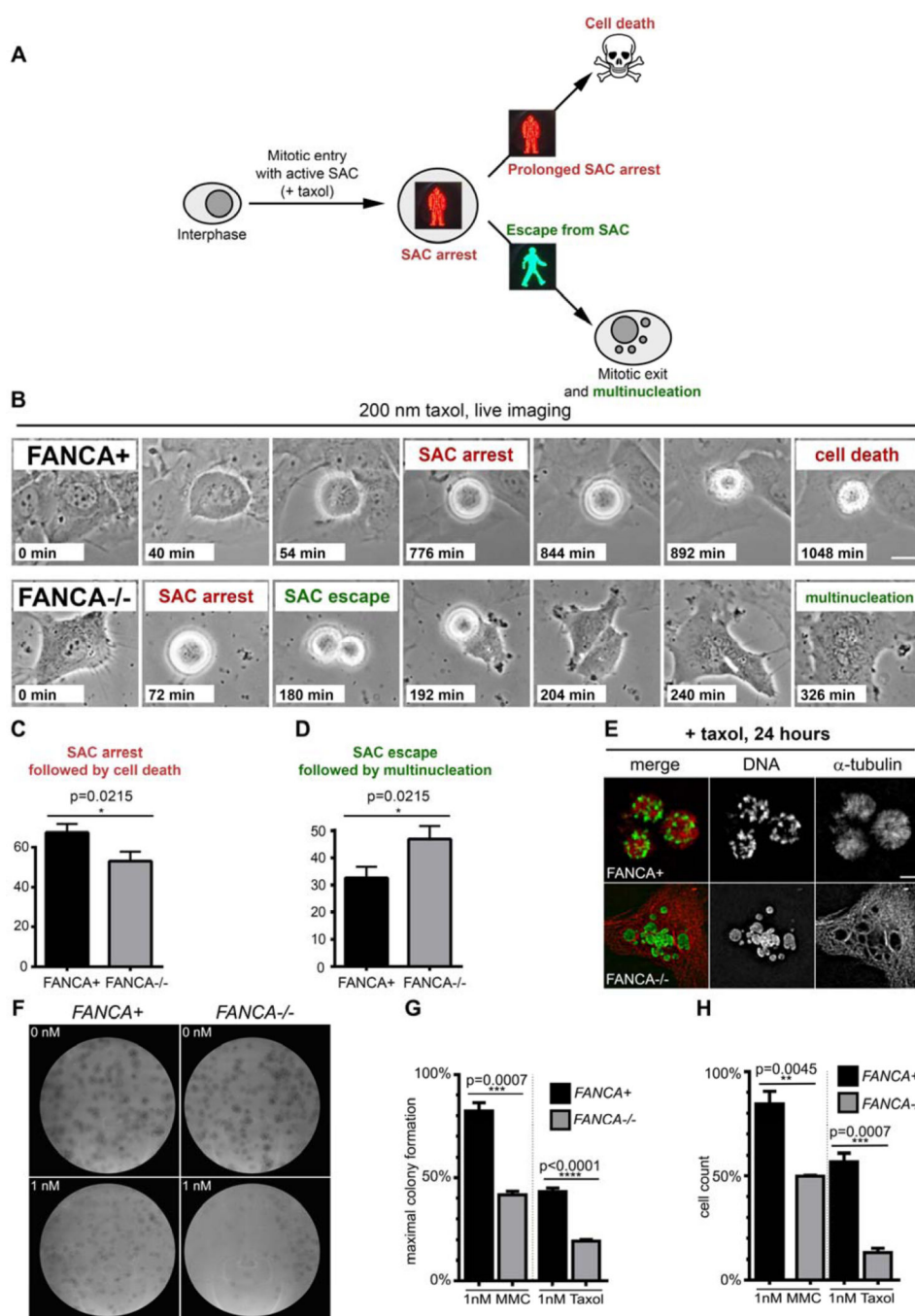


Figure 6. Loss of FANCA promotes escape from SAC and is synthetic lethal with low-dose taxol exposure

(A) Assay schematic. Prolonged activation of SAC triggers cell death to prevent genomic instability by eliminating cells that cannot satisfy the checkpoint. Escape from SAC followed by erratic chromosome segregation and mitotic exit generates multinucleated cells. (B) Representative time-lapse imaging snapshots of *FANCA*⁺ and *FANCA*^{-/-} cells exposed to taxol. Note prolonged SAC arrest followed by cell death in gene-corrected cell and escape for SAC followed by cytokinesis failure and multinucleation in *FANCA*^{-/-} cell. Scale bar:

15 μ m. Time from mitotic entry is shown for each frame. Time-lapse phase-contrast frames of cells grown in DMSO supplemented with 10% FBS at 37°C, 5% CO₂ were acquired every 2 minutes for at least 24 hours on a Nikon Biostation live-imaging system (**C, D**) Quantification of time-lapse imaging experiments. *FANCA*^{-/-} cells are more likely to escape SAC and less likely to be eliminated through SAC-associated death compared to gene-corrected isogenic cells (p=0.0215). Data for 115 mitotic *FANCA*⁺ cells and 129 mitotic *FANCA*^{-/-} cells (three experimental replicates for each cell line) were analyzed with two-tailed t-test. See Supplemental Movies 1–2. (**E**) Prolonged prometaphase arrest in *FANCA*⁺ cells and multinucleation in *FANCA*^{-/-} cells upon 24-hour exposure to taxol in an independent experiment. Images acquired on an Applied Precision personalDx deconvolution microscope. (**F**) Representative colony-forming (CFU) assay plates. Primary *FANCA*^{-/-} fibroblasts and *FANCA*^{+/+} fibroblasts (500 cells per 10 cm² plate) were exposed to taxol for 11 days. Note decreased colony formation on *FANCA*^{-/-} plates exposed to 1 nM of taxol. (**G**) Quantification of the CFU assay shown in (**F**). *FANCA*^{-/-} cells are more sensitive to 1 nM taxol than *FANCA*⁺ cells in the CFU assay. 1 nM MMC was used as positive control. (**H**) Direct cell counts confirm that stable expression of *FANCA* rescues both taxol and MMC hypersensitivity of *FANCA*^{-/-} patient cells. Two-way ANOVA with Sidak correction was used for data comparison. Data show pooled results of three separate experiments, expressed as the mean \pm SEM in triplicates.

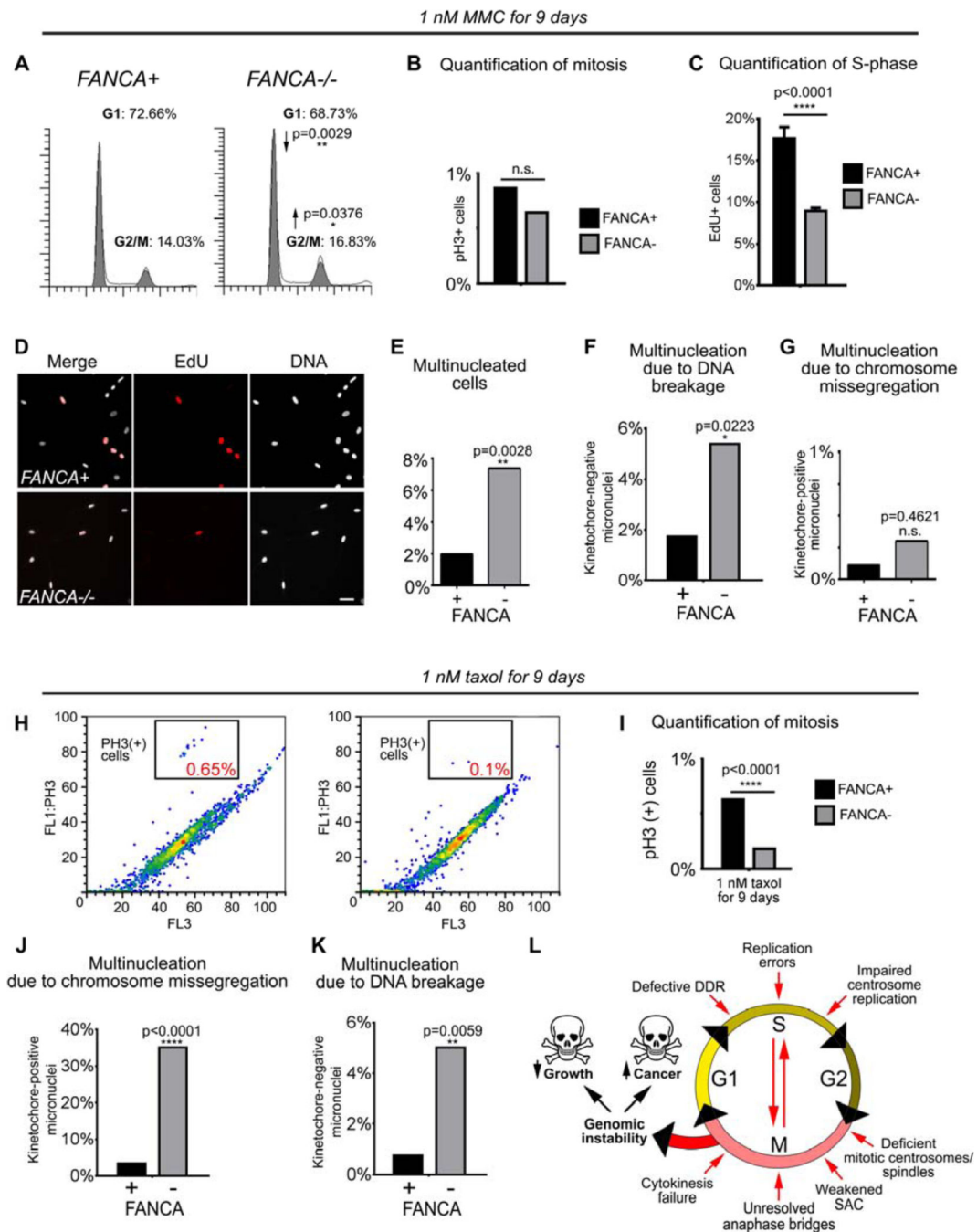


Figure 7. *FANCA*^{-/-} cells exposed to genotoxic stressors develop genomic instability through a combination of interphase and mitotic checkpoint abnormalities

(A) Prolonged activation of the G2/M checkpoint in *FANCA*^{-/-} cells grown in low-dose MMC for 9 days. (B) No difference in mitotic cell fraction between MMC-treated *FANCA*^{-/-} and *FANCA*⁺ cells indicates that the increased *FANCA*^{-/-} G2/M fraction shown in (A) reflects G2 arrest prior to mitotic entry. (C, D) DNA replication arrest in *FANCA*^{-/-} cells exposed to 1 nM MMC is rescued by *FANCA* gene correction. S-phase cells were labeled red by EdU incorporation. (E, F, G) Increased multinucleation due to DNA breakage, but

not chromosome missegregation, in *FANCA*^{-/-} cells grown in low-dose MMC. (**H, I**) Flow cytometry shows decreased fraction of mitotic cells in *FANCA*^{-/-} cells exposed to sublethal dose of taxol. (**J, K**) Treatment with taxol increases chromosome segregation errors and chromosome breakage in *FANCA*^{-/-} cells. (**L**) Compound interphase and mitotic origins of genomic instability in FA-deficient cells (see text for discussion). Exponential accumulation of DNA damage may result in activation of cell cycle arrest/apoptosis (bone marrow failure) or malignant transformation (leukemia and solid tumors). All flow cytometry data represent pooled 3 replicates for each cell line and condition compared with two-tailed t-test. EdU incorporation counts were compared via two-way ANOVA with Sidak's multiple comparisons test.